ChemComm

Accepted Manuscript

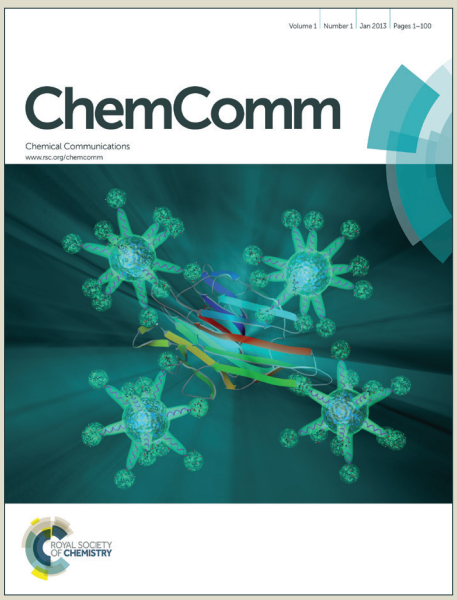

ROYAL SOCIETY OF CHEMISTRY

www.rsc.org/chemcomm

TOC graphic

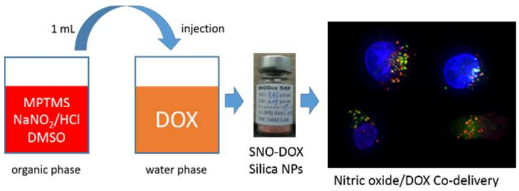

Supramolecular interaction of S-nitroso-polysilsesquioxane and doxorubicin leads to a single nanocarrier for simultaneous intracellular delivery of nitric oxide and doxorubicin.

Chemical Communications

COMMUNICATION

An efficient S-NO-polysilsesquioxane nano-platform for the co-delivery of nitric oxide and an anticancer drug

Meng-Ren Wang[a], Shih-Jiuan Chiu[b], Hung-Chang Chou[a], and Teh-Min Hu*[a]

Received 00th January 20xx,
Accepted 00th January 20xx

DOI: 10.1039/x0xx00000x

www.rsc.org/

Codelivery of nitric oxide (NO) and drugs based on a single nanocarrier is a promising therapeutic strategy. Here, we report a one-step nanoprecipitation method to generate nanoparticles that possess simultaneous NO-donating and doxorubicin release properties. S-nitroso polysilsesquioxane acts like an avid "drug sponge" that attracts drug molecules into nanospheres.

Nitric oxide (NO) plays important roles in physiology and pathophysiology. Recently, NO has been shown to enhance cancer chemotherapy and radiotherapy.[1] NO is a gaseous free radical; thus, exogenous administration of NO mainly relies on NO-donating molecules (NO donors). Previous studies demonstrate that small molecular NO donors can resensitize cancer cells to various anticancer drugs.[2-5] Besides, various NO-releasing nanoparticles (NPs) have been synthesized[6-15] and some of them have been shown to exert antitumor activity.[16-19] In particular, Boyer and Davis et al.[20] successfully attached a physiologically relevant NO donor, S-nitrosoglutathione (GSNO), to polymeric NPs, which substantially enhanced the stability of the intrinsic NO donor. They further demonstrated that combination of the GSNO-based NPs with cisplatin resulted in a synergistic anticancer effect.[20] Although free cisplatin and the NO-releasing NPs were separately administered, the study reveals an important concept that traditional chemotherapy can be augmented with improved NO delivery. Given that the major problem with chemotherapy is the systemic side effects associated with non-selective drug distribution, it is desirable to deliver anticancer drugs using nanoformulations with passive or active targeting capabilities, even in a combination therapy regimen. Therefore, a logical next step is to develop nanoscale NO and drug codelivery systems for cancer therapy (i.e. NO and anticancer drugs are co-encapsulated in the same nanoparticles). However, it is challenging to incorporate two distinct molecules (i.e. NO vs. common organic drug molecule) into one single nanocarriers. Here, we describe an effective method to accomplish this.

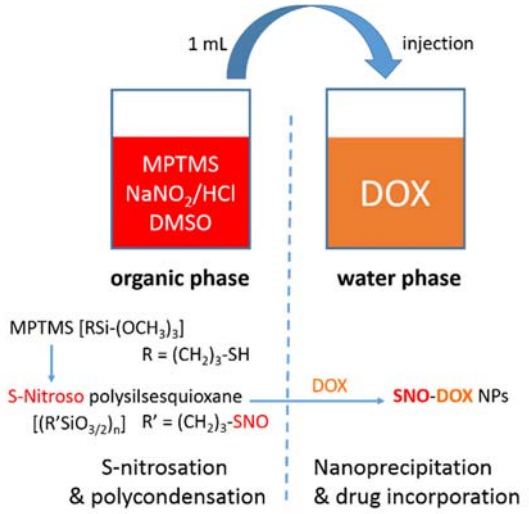

Scheme 1. Schematic representation of the proposed method

Scheme 1 depicts the one-step, simultaneous nanoprecipitation/drug entrapment procedure, in which an organic phase containing S-nitroso (SNO) polysilsesquioxane mixes with a doxorubicin (DOX)-containing water phase by a single rapid injection. SNO-polysilsesquioxane is formed based on acid-catalyzed polycondensation of MPTMS in the presence of sodium nitrite at ambient temperature.[21] After 24 h, the organic phase was injected into the water phase to induce nanoparticle formation and drug encapsulation. In our previous study, we have extensively studied the experimental conditions that would produce the optimal NO-releasing NPs.[21] In the present study, our focus is on how DOX can be co-encapsulated using the previously optimized nanoprecipitation procedure. Upon mixing, the solution immediately become turbid with

[a] School of Pharmacy, National Defense Medical Center, Taipei 11490, Taiwan, ROC.
[b] School of Pharmacy, College of Pharmacy, Taipei Medical University, Taipei 11031, Taiwan, ROC.
*Correspondence: tmhu@ndmctsgh.edu.tw
Electronic Supplementary Information (ESI) available: Materials and Methods, supplementary figures S1-S11. See DOI: 10.1039/x0xx00000x

color changing from pink to orange, with increasing DOX concentrations in the water phase (Figure 1a). The hydrodynamic sizes of formed particles increased nonlinearly with DOX concentrations: a moderate increase at low concentrations vs. a marked increase at the high concentration range (Figure 1a). The dependence of particle sizes on DOX concentrations seemed to follow power-law relationships and there is a criticality point at [DOX] = 80 μM (Figure S1). Below the critical concentration, the particle sizes were below 300 nm and the incremental size was a power function of DOX concentrations with an exponent value of 1.77. Above the critical concentration up to 180 μM, the incremental size had an almost perfect (r=0.999) power-law dependence on DOX concentrations, with a much higher exponent value of 4.04 (Figure S1). The encapsulation efficiency of DOX was measured and the results were reported in Figure 1a. As can be seen, DOX was efficiently entrapped in the nanoparticles; the efficiency reached maximum (~80%) at 60 μM, and decreased gradually with further increasing the concentration, suggesting that the system has been saturated. To further characterize the proposed method, the effect of changing the polycondensation time on particle formation and drug encapsulation was tested. Figure S2 shows that for shorter organic-phase reaction times (e.g., <12 h), the subsequent solvent-water mixing step produced large particles (>1000 nm) with low drug encapsulation. In fact, the sizes of formed particles decreased (see also Figure S3 for size distribution), whereas the encapsulation rates increased, with reaction time; and at 24 h, the system could elicit nanoparticle formation and maximum drug entrapment through mixing the organic phase with the DOX-containing water phase (Figure S2). The results suggest that the degree of silica polycondensation is an important factor governing nanoprecipitation and simultaneous drug incorporation. The solvent used may also determine the extent of silica polymerization and the later nanoprecipitation outcome. To investigate the solvent effect, four different solvents were used to constitute the organic phase. After reaction for 24 h and following the mixing step, particle sizes and encapsulation efficiency were measured and compared. The result shows that DMSO was the most effective solvent, because it generated the smallest particles with the highest drug encapsulation capacity (Figure S4). Next, the effect of placing DOX in the organic phase vs. in the water phase was investigated. Figure S5 indicates that regardless of where DOX was initially placed, nanoprecipitation produced comparable results. This suggests that instantaneous interaction between silica species and DOX during solvent-water intermixing was sufficient to allow for significant drug encapsulation. Finally, we examined whether the final nanoparticle sizes can be fine-tuned by adjusting the solvent property (polarity) of the water phase. As shown in Figure S6, by simply adding a small amount of ethanol into the water phase before nanoprecipitation, the size of formed nanoparticles was increased with ethanol concentrations and can be predicted by a log-linear relationship (Log size = 0.042*[ethanol] + 1.86, r = 0.990). Notably, the drug entrapment was only slighted affected by the presence of ethanol (Figure S7).

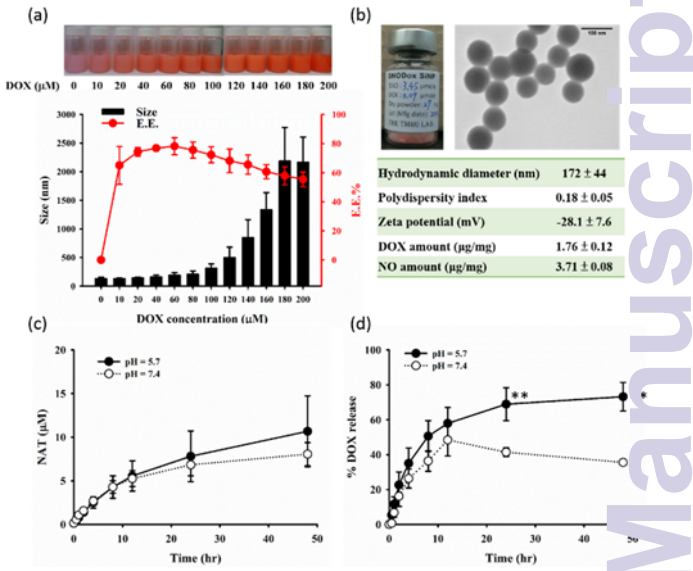

Figure 1. Preparation, characterization, and release of NO-DOX codelivery NPs (i.e. SNODOX). (a) Photo images, hydrodyna... diameters, and encapsulation efficiency (E.E.) of DOX (taken an measured immediately after nanoprecipitation). (b) The fina freeze-dried product, TEM image, and physicochemica properties. (c) Cumulative NO release in PBS-based solution at 37 °C. The measurement was based on the formation of an NO-fluorescent probe adduct (NAT). (d) DOX release as a functio of pH. **P <0.01.

After nanoprecipitation, the colloidal solution was aged at room temperature for 1 h and nanoparticles were collected an purified by repeat wash/centrifugation steps. The fina nanoparticles were redispersed in water containing 5 trehalose for lyophilization. Figure 1b shows the final freeze-dried product and the physicochemical properties of th particles. Here, the formulation is referred to as SNODO (meaning: S-nitroso and DOX co-loaded nanoparticles). As can be seen, SNODOX contains spherical particles with diameters within the range of 50 – 100 nm (TEM). The mean hydrodynam diameter of redispersed particles was 172 nm with good siz distribution (polydispersity = 0.18). The zeta potential was around – 30 mV, which is lower than that of the plain SNO silic nanoparticles reported in our previous study (– 40 mV). Apparently, the incorporation of positively charged DOX ha resulted in slight reduction in surface negative charges. Th amounts of DOX and NO contained in the SNODOX lyophilize powder were determined to be 1,76 μg/mg and 3.71 μg/mg, respectively. The solid-state Si NMR spectrum confirms the silsesquioxane structure by showing almost equally distributed T^2 (–58 ppm) and T^3 (–67 ppm) silicon structure (Figure S8). N and DOX release was studied in PBS-based release medium a pH 7.4 and 5.7. The results show sustained NO and doxorubici co-release for >48 h (Figures 1c, 1d). Particularly, while NO release was pH-independent, DOX release was sensitive to pH showing favorable release at an acidic pH that is tumor environment relevant. The data suggest that SNODOX would

release more DOX in the tumor site than in plasma or normal tissues, which is a desired property for an anticancer drug delivery system. Moreover, the data imply that positively charged DOX interacts electrostatically with the negatively charged silica structure. Finally, for NO-donating property, our further study shows that SNODOX would provide sustained NO release over 7 days (Figure S9).

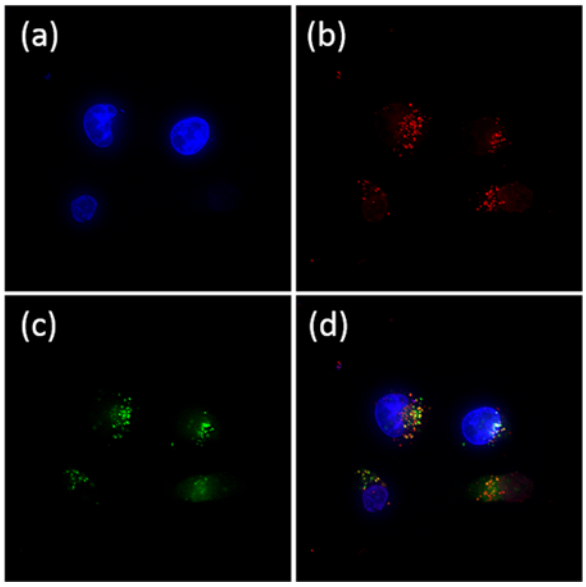

Figure 2. Fluorescence deconvolution microscopy images for cellular uptake of SNODOX NPs in MDA-MB-231 cells. (a) DAPI (for nuclei), (b) DOX, (c) DAF-2DA (for NO), (d) merge. See Figure S10 for complete images and comparisons.

Cellular uptake was studied in a breast cancer cell line (MDA-MB-231) using a fluorescence deconvolution microscopy platform (DeltaVision). A nitric oxide fluorescent probe (DAF-2DA) was used for detecting intracellular NO release.[22] Figure 2 shows the fluorescence images for 24-h cellular translocation of SNODOX NPs (see also Figure S10 for the comparison with free DOX and SNO silica NPs). Remarkably, for SNODOX, cellular codelivery of DOX and NO was manifested by the presence of multicolor dots in the overlapped image (a wide range of colors as a result of the overlapping the three primary colors – red, green, blue). Both DOX and NO signals were mainly co-localized in the perinuclear region, with some nuclear uptake. In contrast, free DOX was completely accumulated in the nucleus (Figure S10). It is important to note that, although SNODOX and free DOX exhibited distinct cellular uptake and intracellular distribution, they showed comparable anticancer effects at 24 and 72 h (Figures 3a, 3b). Incorporation of DOX seemed not to significantly reduce the cytotoxic effect of SNODOX, partly due to the additive anticancer effect of NO. Such a boosting effect is beneficial, because particle encapsulation of DOX often causes a substantial loss of cytotoxicity. The toxicity of SNODOX and free DOX against normal cells was further compared in Figures 3c and 3d. Apparently, SNODOX is less toxic to the H9c2 rat cardiomyoblast cell line than free DOX.

To demonstrate the versatility and generalizability of the proposed method, the same procedure was applied to a fluorescent compound, fluorescein, alone or in combination with DOX at different ratios. As shown in Figure S11, fluorescein-loaded SNO silica NPs (SNOFlu) was successfully prepared with high fluorescein entrapment. Remarkably, both fluorescein and DOX can be simultaneously incorporated into the SNO silica structure at various loading ratios with equal efficiency. Thus, it is an efficient and straightforward method to produce triple-loaded NPs.

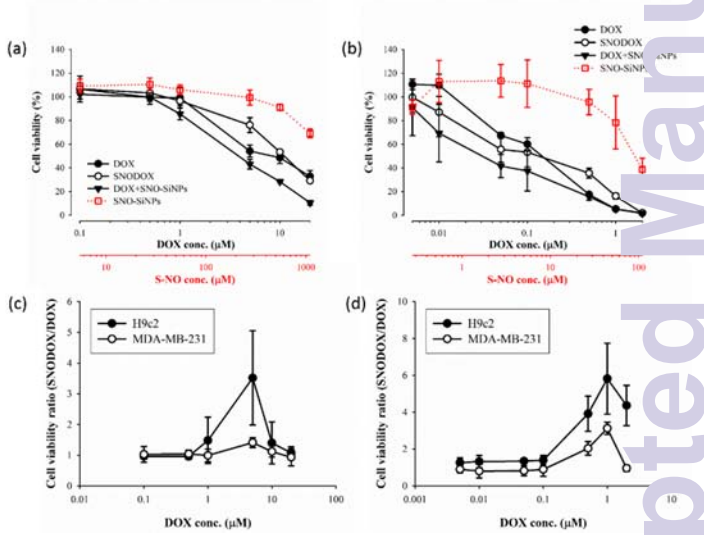

Figure 3. Cytotoxicity of SNODOX. (a) Cell viability measured (MTT assay) at 24 h for MDA-MB-231 cells. (b) Cell viability at 72 h for MDA-MB-231 cells. Comparative cytotoxicity between SNODOX and DOX in H9c2 and MDA-MB-231 cells at (c) 24 h and (d) 72 h.

Conclusions

Nitric oxide (NO) has been implicated in anticancer therapy. In particular, NO enhances the antitumor activity of traditional chemotherapeutic agents. NO is an unstable molecule, and nanocarriers can offer effective NO delivery. Accordingly, a promising new strategy is to achieve codelivery of NO and anticancer drugs using a single nanostructure. Here, we demonstrate for the first time that S-nitroso polysilsesquioxane provides a versatile platform for simultaneous delivery of NO and drugs, focusing on doxorubicin (DOX). The approach is based on a straightforward principle – using the NO-conjugated silica structure to capture drug molecules. Thus, the nanostructure possesses both NO-donating and drug carrying properties. We show that a single injection was effective to produce size-tunable NPs with high drug encapsulation efficiency. Moreover, the method can be applied to other drugs and to incorporate multiple drugs. We envision that the SNO silica species can be broadly tested as a nano "drug sponge" that avidly incorporate drugs and generate NO-drug codelivery systems.

Acknowledgements. The work was supported by the Ministry of Science and Technology (MOST) of Taiwan (NSC 102-2320-B-016-003-MY3). We thank Ms Huei-Min Chen and the Core Facility Center, Office of Research and Development (Taipei Medical University) for the technical support of TEM. We also thank the Instrumentation Center of the National Taiwan University for the solid-state ^{29}Si NMR measurement.

Notes and references

1. A. B. Seabra, R. de Lima and M. Calderon, *Curr Top Med Chem*, 2015, **15**, 298-308.
2. H. Yasuda, K. Nakayama, M. Watanabe, S. Suzuki, H. Fuji, S. Okinaga, A. Kanda, K. Zayasu, T. Sasaki, M. Asada, T. Suzuki, M. Yoshida, S. Yamanda, D. Inoue, T. Kaneta, T. Kondo, Y. Takai, H. Sasaki, K. Yanagihara and M. Yamaya, *Clin Cancer Res*, 2006, **12**, 6748-6757.
3. C. B. Evig, E. E. Kelley, C. J. Weydert, Y. Chu, G. R. Buettner and C. P. Burns, *Nitric Oxide*, 2004, **10**, 119-129.
4. A. Bratasz, N. M. Weir, N. L. Parinandi, J. L. Zweier, R. Sridhar, L. J. Ignarro and P. Kuppusamy, *Proc Natl Acad Sci U S A*, 2006, **103**, 3914-3919.
5. Q. Song, S. Tan, X. Zhuang, Y. Guo, Y. Zhao, T. Wu, Q. Ye, L. Si and Z. Zhang, *Mol Pharm*, 2014, **11**, 4118-4129.
6. J. F. Quinn, M. R. Whittaker and T. P. Davis, *J Control Release*, 2015, **205**, 190-205.
7. A. B. Seabra, G. Z. Justo and P. S. Haddad, *Biotechnol Adv*, 2015.
8. A. W. Carpenter, D. L. Slomberg, K. S. Rao and M. H. Schoenfisch, *ACS Nano*, 2011, **5**, 7235-7244.
9. J. H. Shin and M. H. Schoenfisch, *Chem Mater*, 2008, **20**, 239-249.
10. J. H. Shin, S. K. Metzger and M. H. Schoenfisch, *J Am Chem Soc*, 2007, **129**, 4612-4619.
11. J. Kim, G. Saravanakumar, H. W. Choi, D. Park and W. J. Kim, *J Mater Chem B*, 2014, **2**, 341-356.
12. H. T. Duong, K. Jung, S. K. Kutty, S. Agustina, N. N. Adnan, J. S. Basuki, N. Kumar, T. P. Davis, N. Barraud and C. Boyer, *Biomacromolecules*, 2014, **15**, 2583-2589.
13. P. Nacharaju, C. Tuckman-Vernon, K. E. Maier, J. Chouake, A. Friedman, P. Cabrales and J. M. Friedman, *Nitric Oxide*, 2012, **27**, 150-160.
14. H. T. T. Duong, A. Ho, T. P. Davis and C. Boyer, *J Polym Sci Pol Chem*, 2014, **52**, 2099-2103.
15. H. T. T. Duong, N. N. M. Adnan, N. Barraud, J. S. Basuki, S. K. Kutty, K. Jung, N. Kumar, T. P. Davis and C. Boyer, *J Mater Chem B*, 2014, **2**, 5003-5011.
16. E. V. Stevens, A. W. Carpenter, J. H. Shin, J. Liu, C. J. Der and M. H. Schoenfisch, *Mol Pharm*, 2010, **7**, 775-785.
17. S. Duan, S. Cai, Q. Yang and M. L. Forrest, *Biomaterials*, 2012, **33**, 3243-3253.
18. H. C. Chou, S. J. Chiu and T. M. Hu, *Biomacromolecules*, 2015.
19. P. Sudhesh, K. Tamilarasan, P. Arumugam and S. Berchmans, *ACS Appl Mater Interfaces*, 2013, **5**, 8263-8266.
20. H. T. Duong, Z. M. Kamarudin, R. B. Erlich, Y. Li, M. W. Jones, M. Kavallaris, C. Boyer and T. P. Davis, *Chem Commun (Camb)*, 2013, **49**, 4190-4192.
21. H. C. Chou, S. J. Chiu, Y. L. Liu and T. M. Hu, *Langmuir*, 2014, **30**, 812-822.
22. H. Kojima, N. Nakatsubo, K. Kikuchi, S. Kawahara, Y. Kirino, H. Nagoshi, Y. Hirata and T. Nagano, *Anal Chem*, 1998, **70**, 2446-2453.